
GCT-TTE: GRAPH CONVOLUTIONAL TRANSFORMER FOR TRAVEL TIME ESTIMATION

A PREPRINT

Vladimir Mashurov*
PJSC Sberbank,
Vavilova Street 19, 117312
Moscow, Russia

Vaagn Chopurian*
PJSC Sberbank,
Vavilova Street 19, 117312
Moscow, Russia

Vadim Porvatov*
PJSC Sberbank,
Vavilova Street 19, 117312
Moscow, Russia

Arseny Ivanov
National University of Science and Technology "MISIS",
Lenin Avenue 4, 119049
Moscow, Russia

Natalia Semenova
Artificial Intelligence Research Institute,
Nizhniy Susalnyy Lane 5, 105064
Moscow, Russia
semenova.bn1@gmail.com

June 8, 2023

ABSTRACT

This paper introduces a new transformer-based model for the problem of travel time estimation. The key feature of the proposed GCT-TTE architecture is the utilization of different data modalities capturing different properties of an input path. Along with the extensive study regarding the model configuration, we implemented and evaluated a sufficient number of actual baselines for path-aware and path-blind settings. The conducted computational experiments have confirmed the viability of our pipeline, which outperformed state-of-the-art models on both considered datasets. Additionally, GCT-TTE was deployed as a web service accessible for further experiments with user-defined routes.

Keywords machine learning · graph convolutional networks · transformers · geospatial data · travel time estimation

Introduction

Travel time estimation (TTE) is an actively developing branch of computational logistics that considers the prediction of potential time expenditures for specific types of trips Jenelius and Koutsopoulos [2013], Wu et al. [2020]. With the recent growth of urban environment complexity, such algorithms have become highly demanded both in commercial services and general traffic management Xuegang et al. [2010].

Despite the applied significance of travel time estimation, it still remains a challenging task in the case of ground vehicles. The majority of the currently established algorithms Wang et al. [2021], Derrow-Pinion et al. [2021] tend to utilize specific data modalities in order to capture complex spatio-temporal dependencies influencing the traffic flow. With the recent success of multimodal approaches in adjacent areas of travel demand prediction Chu et al. [2020] and journey planning He et al. [2022], fusing the features from different sources is expected to be the next step towards better performance in TTE.

In this paper, we explored the predictive capabilities of TTE algorithms with different temporal encoders and propose a new transformer-based model GCT-TTE. The main contributions of this study are the following:

1. In order to perform the experiments with the image modality, we extended the graph-based datasets for Abakan and Omsk Porvatov et al. [2022] by the cartographic images in accordance with the provided trajectories.

*These authors contributed equally

Table 1: Demonstration of utilized modalities in path-blind and path-aware models

Path-blind models				Path-aware models			
Model	Modality			Model	Modality		
	Graph	Images	GPS		Graph	Images	GPS
AVG	-	-	-	WDR	+	-	-
LR	-	-	-	DeepIST	-	+	-
MURAT	+	-	-	DeepTTE	-	-	+
DeepI2T	+	+	-	DeepI2T	+	+	-

Currently, the extended datasets are the only publicly available option for experiments with multimodal TTE algorithms.

2. In order to boost further research in the TTE area, we reimplemented and published the considered baselines in a unified format as well as corresponding weights and data preprocessing code. This contribution will enable the community to enhance evaluation quality in the future, as most of the TTE methods lack official implementations.
3. We proposed the GCT-TTE neural network for travel time estimation and extensively studied its generalization ability under various conditions. Obtained results allowed us to conclude that our pipeline achieved better performance regarding the baselines in terms of several metrics.
4. Conducted experiments explicitly indicate that performance of the transformer-based models is less prone to decrease with the scaling of a road network. This property remains crucial from an industrial perspective, as the classic recurrent models undergo considerably larger performance dropdowns.
5. For demonstration purposes, we deployed inference of the GCT-TTE model as the web application accessible for manual experiments.

The web application is available at <http://gctte.online> and the code is published in the GitHub repository of the project¹.

Related work

Travel time estimation methods can be divided into two main types of approaches corresponding to the *path-blind* and *path-aware estimation*, Table 1. The path-blind estimation refers to algorithms relying only on data about the start and end points of a route Wang et al. [2019]. The path-aware models utilize intermediate positions of a moving object represented in the form of GPS sequences Wang et al. [2014], map patches Fu and Lee [2019], or a road subgraph Wang et al. [2021]. Despite the certain computational complexity increase, such approaches provide significantly better results which justify the attention paid to them in the recent studies Zhang et al. [2018], Derrow-Pinion et al. [2021], Sun et al. [2021].

One of the earliest path-aware models was the WDR architecture Wang et al. [2018a] which mostly inherited the concept of joint learning from recommender systems Cheng et al. [2016]. In further studies, this approach was extended regarding the usage of different data modalities. In particular, the DeepIST Fu and Lee [2019] model utilizes rectangular fragments of a general reference map corresponding to elements of a route GPS sequence. Extracted images are fed into a convolutional neural network (CNN) that captures spatial patterns of depicted infrastructure. These feature representations are further concatenated into the matrix processed by the LSTM-based temporal layer Hochreiter et al. [1997].

In contrast with the other approaches, DeepTTE Wang et al. [2018b] is designed to operate directly on GPS coordinates via geospatial convolutions paired with a recurrent neural network. The first part of this pipeline transforms raw GPS sequences into a series of feature maps capturing the local spatial correlation between consecutive coordinates. The final block learns the temporal relations of obtained feature maps and produces predictions for the entire route along with its separate segments.

The concept of modality fusing was first introduced in TTE as a part of the DeepI2T Lan et al. [2019] model. This architecture utilizes LINE Tang et al. [2015] to produce grid embeddings and 3-layer CNN with pooling for image

¹<https://github.com/Eighonet/GCT-TTE>

representations. As well as DeppTTE, DeepI2T includes the segment-based prediction component implemented in the form of residual blocks on the top of the Bi-LSTM encoder.

In addition to extensively studied recurrent TTE methods, it is also important to mention recently emerged transformer models Liu et al. [2022], Semenova et al. [2022]. Despite the limited comparison with classic LSTM-based methods, they have already demonstrated promising prediction quality, preserving the potential for further major improvements Shen et al. [2022], Fan et al. [2021]. As most of the transformer models lack a comprehensive evaluation, we intend to explore GCT-TTE performance with respect to a sufficient number of state-of-the-art solutions to reveal its capabilities explicitly.

Preliminaries

In this section, we introduce the main concepts required to operate with the proposed model.

Route. A route r is defined as the set $\{c^r, a^r, t^r\}$, where c^r is the sequence of GPS coordinates of a moving object, a^r is the vector of temporal and weather data, t^r is the travel time.

As the *image modality* p^r of a route r , we utilize geographical map patches corresponding to each coordinate $c_i^r \in c^r$. Each image has a fixed size $W \times H \times 3$ across all of the GPS sequences in a specific dataset.

Road network. Road network is represented in the form of graph $G = \{V, E, X\}$, where $V = \{v_1, \dots, v_n\}$ is the set of nodes corresponding to the segments of city roads, $E = \{(v_i, v_j) \mid v_i \rightarrow v_j\}$ is the set of edges between connected nodes $v_i, v_j \in V$, $X : n \times m \rightarrow \mathbf{R}$ is a feature matrix of nodes.

Description of a route r can be further extended by the *graph modality* $g^r = \{v_k \mid k = \arg\min_j \rho(c_i^r, v_j)\}_{i=1}^{|c^r|}$, where $\rho(c_i^r, v_j)$ is the minimum Euclidean distance between coordinates associated with v_j and c_i^r .

Travel time estimation. For each entry r , it is required to estimate the travel time t^r using the elements of feature description $\{c^r, p^r, g^r, a^r\}$.

Data

We explored the predictive performance of the algorithm on two real-world datasets collected during the period from December 1, 2020 to December 31, 2020 in Abakan (112.4 square kilometers) and Omsk (577.9 square kilometers). Each dataset consists of a road graph and associated routes, Table 2. In the preprocessing stage, we excluded trips that lasted less than 30 seconds along with the ones that took more than 50 minutes.

In order to supply the image-based models with the relevant input data, we extended the road graphs with the map patches parsed via Open Street Map API². Depending on the requirements of the considered learning model, image datasets had to be constructed regarding the fixed grid partitions or centered around the elements of GPS sequences. In the first case, a geographical map of a city was divided into equal disjoint patches, which were further mapped with the GPS data in accordance with the presence of coordinates in a specific partition. Trajectory-based approach to dataset construction does not require the disjoint property of images and relies on the extraction of patches with the center in the specified coordinate. The obtained grid-based image dataset consists of 96 101 instances for Abakan and 838 865 for Omsk while the trajectory-based dataset has 544 502 and 3 376 294 images correspondingly.

One of the crucial features of the considered datasets is the absence of traffic flow properties. The availability of such data is directly related to the specialized tracking systems (based on loop detectors or observation cameras), which are not presented in the majority of cities. In order to make the GCT-TTE suitable for the greatest number of urban environments, we decided not to limit the study by the rarely accessible data.

Method

In this section, we provide an extensive description of the GCT-TTE main components: pointwise and sequence representation blocks, Figure 1.

²<https://www.openstreetmap.org>

Table 2: Description of the Abakan and Omsk datasets.

Road network			Trips		
Property \ City	Abakan	Omsk	Property \ City	Abakan	Omsk
Nodes	65 524	231 688	Trips number	121 557	767 343
Edges	340 012	1 149 492	Coverage	53.3%	49.5%
Clustering	0.5278	0.53	Average time	427 sec	608 sec
Usage median	12	8	Average length	3604 m	4216 m

Patches encoder

In order to extract features from the image modality, we utilized the RegNetY Radosavovic et al. [2020] architecture from the SEER model family. The key component of this architecture is the convolutional recurrent neural network (ConvRNN) which controls the spatio-temporal information flow between building blocks of the neural network.

Each RegNetY block consists of three operators. The initial convolution layer of t 'th block processes the input tensor X_1^t and returns the feature map X_2^t . Next, the obtained representation X_2^t is fed to ConvRNN:

$$H^t = \tanh(C_x(X_2^t) + C_h(H^{t-1}) + b_h), \quad (1)$$

where H^{t-1} is the hidden state of the previous RegNetY block, b_h is a bias tensor, C_x and C_h correspond to convolutional layers. In the following stage, X_2^t and H^t are utilized as input of the last convolution layer, which is further extended by residual connection.

As the SEER models are capable of producing robust features that are well-suited for out-of-distribution generalization Goyal et al. [2022], we pre-trained RegNetY with the following autoencoder loss:

$$\mathcal{L}(W \times \text{RegNet}(X), f(X)) \rightarrow 0, \quad (2)$$

where \mathcal{L} is the binary cross-entropy function, f is an image flattening operator, and W is the projection matrix of learning parameters that maps model output to the flattened image.

Auxiliary encoder

Along with the map patches and graph elements, we apply additional features a^r corresponding to the temporal and weather data (e.g., trip hour, type of day, precipitation). The GCT-TTE model processes this part of the input with the help of a trivial linear layer:

$$A^r = W a^r, \quad (3)$$

where W is a matrix of learning parameters.

Graph encoder

The graph data is handled with the help of the graph convolutional layers Kipf and Welling [2016] defined as follows:

$$h_u^{(k)} = \text{ReLU} \left(W^{(k)} \text{AGG}_{v \in \mathcal{N}(u)} \left(\frac{h_v^{(k-1)}}{|\mathcal{N}_{uv}|} \right) \right), \quad (4)$$

where $h_u^{(k)}$ is a k -hop embedding of $u \in V$, $h_u^{(0)} = x_u$, $W^{(k)}$ is a matrix of learning parameters of k 'th convolutional layer, $\mathcal{N}(u)$ is a set of neighbour nodes of u , $\text{AGG}_{v \in \mathcal{N}(u)}$ is a sum aggregation function, and $|\mathcal{N}_{uv}| = \sqrt{|\mathcal{N}(u)||\mathcal{N}(v)|}$.

To accelerate the convergence of the GCT-TTE model, we pre-trained the weights of the graph convolutions by the Deep Graph InfoMax algorithm Veličković et al. [2019]. This approach optimizes the loss function that allows learning the difference between initial and corrupted embeddings of nodes:

$$\mathcal{L} = \frac{1}{N+M} \left(\sum_{i=1}^N E_{\mathcal{G}} \left[\log(D(h_u, h_{\mathcal{G}})) \right] + \sum_{j=1}^M E_{\tilde{\mathcal{G}}} \left[\log(1 - D(\tilde{h}_u, h_{\mathcal{G}})) \right] \right), \quad (5)$$

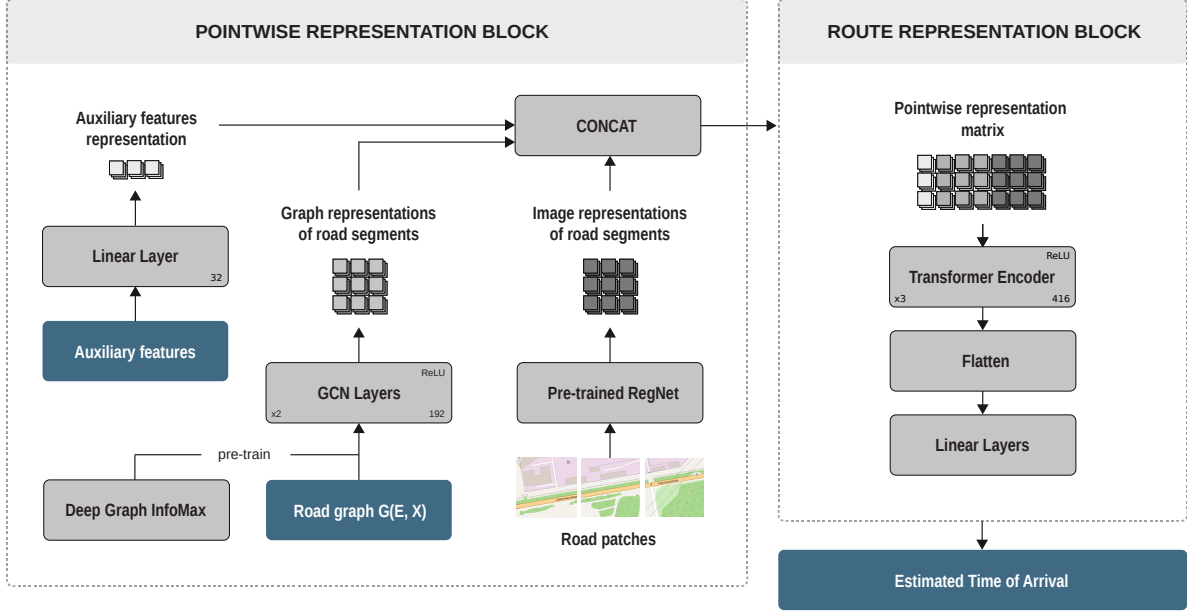


Figure 1: Demonstration of the GCT-TTE pipeline.

where h_u is an embedding of node u based on the initial graph \mathcal{G} , \tilde{h}_u is an embedding of a node u from the corrupted version $\tilde{\mathcal{G}}$ of the graph \mathcal{G} , D corresponds to the discriminator function.

The final output of the pointwise block constitutes a concatenation of the weighted representations and auxiliary data for each route r with k segments:

$$P_r = \text{CONCAT}(\alpha \cdot H^r, (1 - \alpha) \cdot I^r, \beta \cdot A^r), \quad (6)$$

where H^r is the matrix of size $k \times e_g$ of graph-based segment embeddings, I^r is the matrix of size $k \times e_i$ obtained from a flattened RegNet output, α , $(1 - \alpha)$, and β correspond to the weight coefficients of specific modalities.

Sequence representation block

To extract sequential features from the output of the pointwise representation block, it is fed to transformer encoder Vaswani et al. [2017]. The encoder consists of two attention layers with a residual connection followed by a normalization operator. The multi-head attention coefficients are defined as follows:

$$\alpha_{i,j}^{(h)} = \text{softmax}_{w_j} \left(\frac{\langle W_{h,q}^T x_i, W_{h,k}^T x_j \rangle}{\sqrt{d_k}} \right), \quad (7)$$

where $x_i, x_j \in P_r$, h is an attention head, d_k is a scale coefficient, $W_{h,q}^T$ and $W_{h,k}^T$ are query and key weight matrices, w_j is a vector of softmax learning parameters. The output of the attention layer will be:

$$u_i = \text{LayerNorm} \left(x_i + \sum_{h=1}^H W_{c,h}^T \sum_{j=1}^n \alpha_{i,j}^{(h)} W_{h,v}^T x_j \right), \quad (8)$$

where $W_{h,v}^T$ is value weight matrix, H is a number of attention heads.

The final part of the sequence representation block corresponds to the flattening operator and several linear layers with the ReLU activation, which predict the travel time of a route.

Results

In this section, we reveal the parameter dependencies of the model and compare the results of the considered baselines.

Experimental setup

The experiments were conducted on 16 GPU Tesla V100. For the GCT-TTE training, Adam optimizer Kingma and Ba [2014] was chosen with a learning rate $5 \cdot 10^{-5}$ and batch size of 16. For better convergence, we apply the scheduler with patience equal to 10 epochs and 0.1 scaling factor. The training time for the final configuration of the GCT-TTE model is 6 hours in the case of Abakan and 30 for Omsk.

The established values of quality metrics were obtained from the 5-fold cross-validation procedure. As the measures of the model performance, we utilize mean absolute error (MAE), rooted mean squared error (RMSE), and 10% satisfaction rate (SR). Additionally, we compute mean absolute percentage error (MAPE) as it is frequently used in related studies.

Models comparison and evaluation

The results regarding path-blind evaluation are depicted in Table 3. Neighbor average (AVG) and linear regression (LR) demonstrated the worst results among the trivial baselines as long as gradient boosted decision trees (GBDT) explicitly outperformed more complex models in the case of the largest city. The MURAT model achieved the best score for Abakan in terms of MAE and RMSE, while GCT-TTE has the minimum MAPE among all of the considered architectures.

Demonstrated variability of metric values makes the identification of the best model rather a hard task for a path-blind setting. The simplest models are still capable to be competitive regarding such architectures as MURAT, which was expected to perform tangibly better on both considered datasets. The results regarding GCT-TTE can be partially explained by its structure as it was not initially designed for a path-blind evaluation.

As can be seen in Table 4, the proposed solution outperformed baselines in terms of the RMSE value, which proves the rigidity of GCT-TTE towards large errors prevention. The comparison of MAE and RMSE for considered methods has shown a minimal gap between these metrics in the case of GCT-TTE for both cities, signifying the efficiency of the technique with respect to dataset size. Overall, the results have confirmed that GCT-TTE appeared to be a more reliable approach than the LSTM-based models: while MAPE remains approximately the same across top-performing architectures, GCT-TTE achieves significantly better MAE and RMSE values. Conducted computational experiments also indicated that DeepI2T and WDR have intrinsic problems with the convergence, while GCT-TTE demonstrates smoother training dynamics.

Performance analysis

In the case of both datasets, dependencies between the travelled distance and obtained MAE on the corresponding trips reveal similar dynamics: as the path length increases, the error rate continues to grow, Figure 2(b, d). The prediction variance is inversely proportional to the number of routes in a particular length interval except for the small percentage of the shortest routes. The main difference between the MAE curves is reflected in the higher magnitudes of performance fluctuations in Abakan compared to Omsk.

The temporal dynamics of GCT-TTE errors exhibit rich nonlinear properties during a 24-hour period. The shape of the error curves demonstrates that our model tends to accumulate a majority of errors in the period between 16:00 and 18:00, Figure 2(a, c). This time interval corresponds to the end of the working day, which has a crucial impact on the traffic flow foreseeability.

Despite the mentioned performance outlier, the general behaviour of temporal dependencies allows concluding that GCT-TTE successfully captures the factors influencing the target value in the daytime. With the growing sparsity of data during night hours, it is still capable of producing relevant predictions for Omsk. In the case of Abakan, the GCT-TTE performance drop can be associated with a substantial reduction in intercity trips number (which emerged to be an easier target for the model).

Sensitivity analysis

In order to achieve better prediction quality, we extensively studied the dependencies between GCT-TTE parameters and model performance in the sense of the MAE metric. The best value for modality coefficient α was 0.9, which reflects the significant contribution of graph data towards error reduction. For the final model, we utilized 2 graph convolutional layers with hidden size 192, Figure 3(a, b). The lack of aggregation depth can significantly reduce the performance of GCT-TTE, while the excessive number of layers has a less expressive negative impact on MAE. A similar situation can be observed in the case of the hidden size, which is getting close to a plateau after reaching a certain threshold value.

Table 3: Path-blind models comparison

<i>Baseline \ Metric</i>	Abakan				Omsk			
	MAE	RMSE	MAPE	SR	MAE	RMSE	MAPE	SR
AVG	322.77	477.61	0.761	0.018	439.05	628.75	0.741	0.012
LR	262.33	456.63	1.169	9.527	416.81	593.01	1.399	7.187
GBDT	245.77	433.91	1.106	10.28	209.99	372.11	0.656	17.72
MURAT	182.97	282.15	0.685	10.77	285.72	444.74	0.856	9.997
GCT-TTE	221.71	337.59	0.505	11.12	376.74	590.93	0.5486	8.99

Table 4: Path-aware models comparison

<i>Baseline \ Metric</i>	Abakan				Omsk			
	MAE	RMSE	MAPE	SR	MAE	RMSE	MAPE	SR
DeepIST	153.88	241.29	0.3905	18.08	256.50	415.16	0.6361	14.39
DeepTTE	111.03	174.56	0.2165	31.45	179.07	296.98	0.1898	34.03
GridLSTM	100.27	206.91	0.2202	30.74	135.74	257.18	0.2120	31.21
DeepI2T	97.99	201.33	0.2128	31.34	136.66	260.90	0.2124	31.23
WDR	97.22	190.09	0.2162	31.98	131.57	269.00	0.2039	33.34
GCT-TTE	92.26	147.89	0.2262	30.46	107.97	169.15	0.1961	35.17

Along with the graph convolutions, we explored the configuration of the sequence representation part of GCT-TTE. Since the transformer block remains its main component, the computational experiments were focused on the influence of encoder depth on quality metrics, Figure 3(c). As it can be derived from the U-shaped dependency, the best number of attention layers is 3.

Demonstration

In order to provide access to the inference of GCT-TTE, we deployed a demonstrational application² in a website format, Figure 4. The application’s interface consists of a user guide, navigation buttons, erase button, and a comparison button. A potential user can construct and evaluate an arbitrary route by clicking on the map at the desired start and end points: the system’s response will contain the shortest path and the corresponding value of the estimated time of arrival.

For additional evaluation of considered baselines, the limited number of predefined trajectories with known ground truth can also be requested. In this case, the response will contain three random trajectories from the datasets with associated predictions of WDR, DeepI2T, and GCT-TTE models along with the real travel time.

Conclusion

In this paper, we introduced a multimodal transformer architecture for travel time estimation and performed an extensive comparison with the other existing approaches. Obtained results allow us to conclude that the transformer-based models can be efficiently utilized as sequence encoders in the path-aware setting. Our experiments with different data modalities revealed the superior importance of graphs compared to map patches. Such an outcome can be explained by the inheritance of main features between modalities where graph data represents the same properties more explicitly. In

²<http://gctte.online>

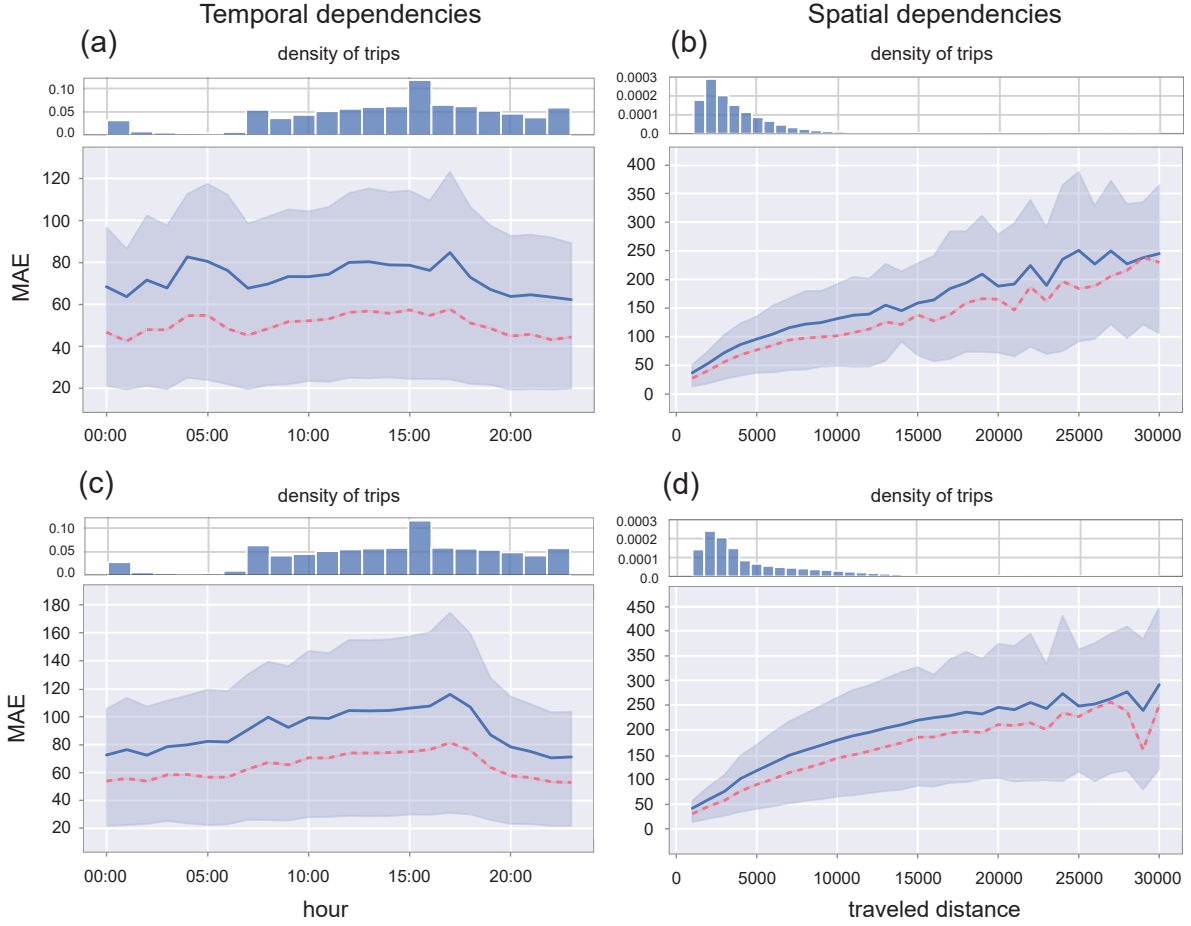


Figure 2: Spatial and temporal dependencies across the different groups of test entries for Abakan (a, b) and Omsk (c, d): blue and red lines depict mean and median values of MAE, borders of filled area correspond to Q1 and Q3 quartiles of a MAE distribution.

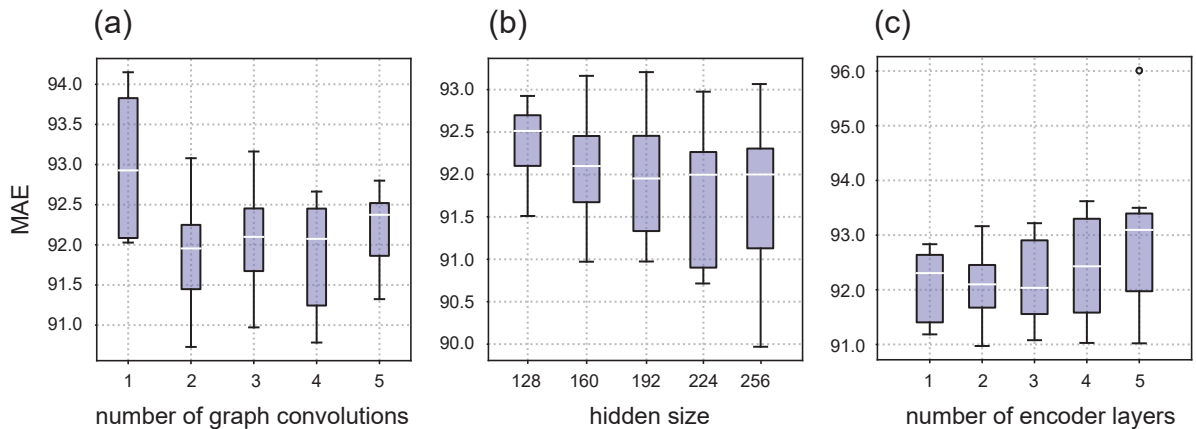


Figure 3: Parametric dependencies of GCT-TTE performance for Abakan: number of graph convolutions (a), hidden size of graph convolutions (b), and number of transformer encoder layers (c).

further studies, we intend to focus on the design of a more expressive image encoder as well as consider the task of path-blind travel time estimation, which currently remains challenging for the GCT-TTE model.

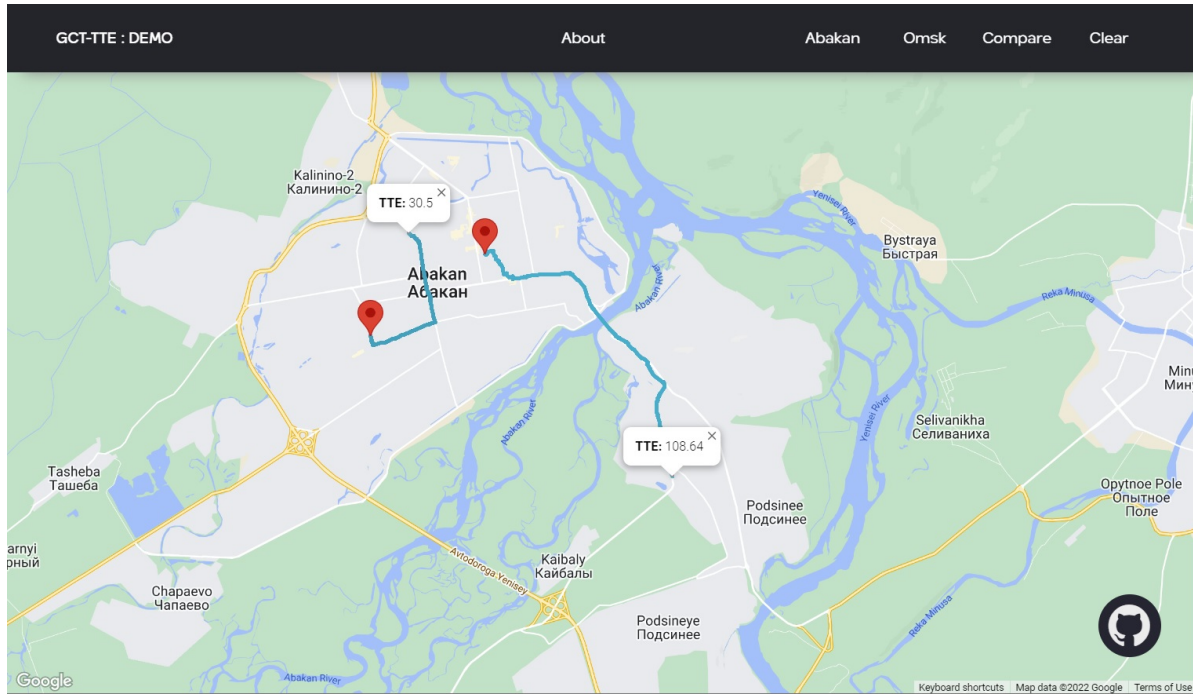


Figure 4: An interface of the demonstrational application.

Declarations

Ethics approval and consent to participate

Not applicable.

Consent for publication

Not applicable.

Availability of data and materials

Considered models and datasets are available in the project’s GitHub repository.

Competing interests

The authors declare that they have no competing interests.

Funding

Not applicable.

Authors contributions

V.M., V.C., and A.I.: Software, Data curation, Validation, Visualization; V.P.: Software, Visualization, Conceptualization, Methodology, Writing (original draft); N.S.: Conceptualization, Methodology, Supervision, Writing (review & editing).

Acknowledgements

The authors are grateful to Vladislav Zamkovy for the help with application deployment.

References

- Erik Jenelius and Haris Koutsopoulos. Travel time estimation for urban road networks using low frequency probe vehicle data. *Transportation Research Part B: Methodological*, 53:64–81, 06 2013.
- Xing Wu, Uttara Roy, Maryam Hamidi, and Brian Craig. Estimate travel time of ships in narrow channel based on ais data. *Ocean Engineering*, 202:106790, 04 2020.
- Jeff Xuegang, Xuegang (Jeff) Ban, Yuwei Li, Alexander Skabardonis, and Jd Margulici. Performance evaluation of travel time estimation methods for real-time traffic applications. *Intelligent Transportation Systems Journal*, 14: 54–67, 04 2010.
- Qiang Wang, Chen Xu, Wenqi Zhang, and Jingjing Li. Graphtte: Travel time estimation based on attention-spatiotemporal graphs. *IEEE Signal Processing Letters*, 28:239–243, 2021.
- Austin Derrow-Pinion, Jennifer She, David Wong, Oliver Lange, Todd Hester, Luis Perez, Marc Nunkesser, Seongjae Lee, Xueying Guo, Brett Wiltshire, et al. Eta prediction with graph neural networks in google maps. In *Proceedings of the 30th ACM International Conference on Information & Knowledge Management*, pages 3767–3776, 2021.
- Kai-Fung Chu, Albert Y. S. Lam, and Victor O. K. Li. Deep multi-scale convolutional lstm network for travel demand and origin-destination predictions. *IEEE Transactions on Intelligent Transportation Systems*, 21(8):3219–3232, 2020. doi:10.1109/TITS.2019.2924971.
- Peilan He, Guiyuan Jiang, Siew-Kei Lam, Yidan Sun, and Fangxin Ning. Exploring public transport transfer opportunities for pareto search of multicriteria journeys. *IEEE Transactions on Intelligent Transportation Systems*, 23(12): 22895–22908, 2022. doi:10.1109/TITS.2022.3194523.
- Vadim Porvatov, Natalia Semenova, and Andrey Chertok. Hybrid graph embedding techniques in estimated time of arrival task. In Rosa Maria Benito, Chantal Cherifi, Hocine Cherifi, Esteban Moro, Luis M. Rocha, and Marta Sales-Pardo, editors, *Complex Networks & Their Applications X*, pages 575–586, Cham, 2022. Springer International Publishing.
- Hongjian Wang, Xianfeng Tang, Yu-Hsuan Kuo, Daniel Kifer, and Zhenhui Li. A simple baseline for travel time estimation using large-scale trip data. *ACM Transactions on Intelligent Systems and Technology (TIST)*, 10(2):1–22, 2019.
- Yilun Wang, Yu Zheng, and Yexiang Xue. Travel time estimation of a path using sparse trajectories. In *Proceedings of the 20th ACM SIGKDD International Conference on Knowledge Discovery and Data Mining*, KDD ’14, page 25–34, New York, NY, USA, 2014. Association for Computing Machinery. ISBN 9781450329569.
- Tao-yang Fu and Wang-Chien Lee. Deepist: Deep image-based spatio-temporal network for travel time estimation. In *Proceedings of the 28th ACM International Conference on Information and Knowledge Management*, CIKM ’19, page 69–78, New York, NY, USA, 2019. Association for Computing Machinery. ISBN 9781450369763.
- Hanyuan Zhang, Hao Wu, Weiwei Sun, and Baihua Zheng. Deeptravel: a neural network based travel time estimation model with auxiliary supervision. In *Proceedings of the 27th International Joint Conference on Artificial Intelligence*, pages 3655–3661, 2018.
- Yiwen Sun, Kun Fu, Zheng Wang, Changshui Zhang, and Jieping Ye. Road network metric learning for estimated time of arrival. In *2020 25th International Conference On Pattern Recognition (ICPR)*, pages 1820–1827. IEEE, 2021.
- Zheng Wang, Kun Fu, and Jieping Ye. Learning to estimate the travel time. In *Proceedings of the 24th ACM SIGKDD International Conference on Knowledge Discovery and Data Mining*, KDD ’18, page 858–866, New York, NY, USA, 2018a. Association for Computing Machinery. ISBN 9781450355520.
- Heng-Tze Cheng, Levent Koc, Jeremiah Harmsen, Tal Shaked, Tushar Chandra, Hrishi Aradhye, Glen Anderson, Greg Corrado, Wei Chai, Mustafa Ispir, et al. Wide & deep learning for recommender systems. In *Proceedings of the 1st workshop on deep learning for recommender systems*, pages 7–10, 2016.
- Sepp Hochreiter, Jürgen Schmidhuber, and Corso Elvezia. Long short-term memory. *Neural Computation*, 9(8): 1735–1780, 1997.
- Dong Wang, Junbo Zhang, Wei Cao, Jian Li, and Yu Zheng. When will you arrive? estimating travel time based on deep neural networks. In *AAAI 2018*, January 2018b.

- Wuwei Lan, Yanyan Xu, and Bin Zhao. Travel time estimation without road networks: An urban morphological layout representation approach. In *Proceedings of the 28th International Joint Conference on Artificial Intelligence, IJCAI'19*, page 1772–1778. AAAI Press, 2019. ISBN 9780999241141.
- Jian Tang, Meng Qu, Mingzhe Wang, Ming Zhang, Jun Yan, and Qiaozhu Mei. Line: Large-scale information network embedding. In *Proceedings of the 24th international conference on world wide web*, pages 1067–1077, 2015.
- Fengkai Liu, Jianhua Yang, Mu Li, and Kuo Wang. Mct-tte: Travel time estimation based on transformer and convolution neural networks. *Scientific Programming*, 2022:3235717, Apr 2022.
- Natalia Semenova, Vadim Porvatov, Vladislav Tishin, Artyom Sosedka, and Vladislav Zamkovoy. Logistics, graphs, and transformers: Towards improving travel time estimation. *arXiv preprint arXiv:2207.05835*, 2022.
- Yibin Shen, Cheqing Jin, Jiaxun Hua, and Dingjiang Huang. Ttpnet: A neural network for travel time prediction based on tensor decomposition and graph embedding. *IEEE Transactions on Knowledge and Data Engineering*, 34(9): 4514–4526, 2022. doi:10.1109/TKDE.2020.3038259.
- Shizhen Fan, Jianbo Li, Zhiqiang Lv, and Aite Zhao. Multimodal traffic travel time prediction. In *2021 International Joint Conference on Neural Networks (IJCNN)*, pages 1–9, 2021. doi:10.1109/IJCNN52387.2021.9533356.
- Ilija Radosavovic, Raj Prateek Kosaraju, Ross Girshick, Kaiming He, and Piotr Dollar. Designing network design spaces. In *Proceedings of the IEEE/CVF Conference on Computer Vision and Pattern Recognition (CVPR)*, June 2020.
- Priya Goyal, Quentin Duval, Isaac Seessel, Mathilde Caron, Ishan Misra, Levent Sagun, Armand Joulin, and Piotr Bojanowski. Vision models are more robust and fair when pretrained on uncurated images without supervision, 2022.
- Thomas N. Kipf and Max Welling. Semi-supervised classification with graph convolutional networks, 2016.
- Petar Veličković, William Fedus, William L. Hamilton, Pietro Liò, Yoshua Bengio, and R Devon Hjelm. Deep Graph Infomax. In *International Conference on Learning Representations*, 2019.
- Ashish Vaswani, Noam Shazeer, Niki Parmar, Jakob Uszkoreit, Llion Jones, Aidan N Gomez, Łukasz Kaiser, and Illia Polosukhin. Attention is all you need. In I. Guyon, U. Von Luxburg, S. Bengio, H. Wallach, R. Fergus, S. Vishwanathan, and R. Garnett, editors, *Advances in Neural Information Processing Systems*, volume 30. Curran Associates, Inc., 2017.
- Diederik Kingma and Jimmy Ba. Adam: A method for stochastic optimization. *International Conference on Learning Representations*, 12 2014.